

RSC Advances



This is an *Accepted Manuscript*, which has been through the Royal Society of Chemistry peer review process and has been accepted for publication.

Accepted Manuscripts are published online shortly after acceptance, before technical editing, formatting and proof reading. Using this free service, authors can make their results available to the community, in citable form, before we publish the edited article. This *Accepted Manuscript* will be replaced by the edited, formatted and paginated article as soon as this is available.

You can find more information about *Accepted Manuscripts* in the [Information for Authors](#).

Please note that technical editing may introduce minor changes to the text and/or graphics, which may alter content. The journal's standard [Terms & Conditions](#) and the [Ethical guidelines](#) still apply. In no event shall the Royal Society of Chemistry be held responsible for any errors or omissions in this *Accepted Manuscript* or any consequences arising from the use of any information it contains.

Effects of Plasticizers on the Strain-Induced Crystallization and Mechanical Properties of Natural Rubber and Synthetic Polyisoprene

Yueqing Ren^{a,b}, Suhe Zhao^{a,b,*}, Qian Yao^{a,b}, Qianqian Li^{a,b}, Xingying Zhang^b, Liqun Zhang^{a,b}

^a *State Key Laboratory of Organic-Inorganic Composites, Beijing University of Chemical Technology, Beijing 100029, P R China*

^b *Key Laboratory of Beijing City on Preparation and Processing of Novel Polymer Materials, Beijing 100029, PR China*

Corresponding Author Footnote: Correspondences should be addressed to Prof. Suhe Zhao*

Phone: +86-10-6444-2621. Fax: +86-10-6443-3964. E-mail: zhaosh@mail.buct.edu.cn.

Abstract: Effects of liquid isoprene (LIR-50) and naphthenic oil (NPO) on the strain-induced crystallization (SIC) measured by in situ synchrotron wide-angle X-ray diffraction (WAXD) and mechanical properties of vulcanized natural rubber (NR) and synthetic polyisoprene (IR) were studied. The onset strain (α_c) of SIC of NR and IR was 250% and 350% respectively. NR and IR exhibited stress upturns at strain 383% and 450% in stress-strain curves, and the crystallinities of NR and IR were 7.6% and 8.6%, respectively. After vulcanization, LIR-50 became part of the rubber network, while NPO still existed as free small molecules in rubber networks. After the respective addition of LIR-50 and NPO, the α_c of NR composites rarely changed, while the α_c of IR composites increased. In addition, the crystallinity and tensile strength of NR and IR filled with LIR-50 and NPO respectively decreased, and the reduction in IR composites was higher than that in NR composites. The crystallinity and mechanical properties of the NR and IR plasticized by LIR-50 respectively were higher than those plasticized by NPO. The maintenance of high crystallinity of NR or IR composites may ensure their good mechanical properties. Therefore, LIR-50 can be used as a reactive plasticizer to maintain good mechanical properties for NR and IR.

Keywords: Plasticizers, Natural rubber, Synthetic polyisoprene, Strain-induced crystallization, Mechanical properties

1. Introduction

Natural rubber (NR) is an indispensable elastomeric material in the rubber industry, and NR consist of more than 99.9% cis-1,4 polyisoprene. The high stereoregularity of NR allows its molecules to orientate along the stretching direction and crystallize when the strain exceeds a critical value (defined as the onset strain (α_c) of crystallization) during stretching.¹ This phenomenon, which is known as strain-induced crystallization (SIC),²⁻⁴ imparts NR with a self-reinforcing characteristic.⁵⁻⁷ Therefore, NR exhibits excellent physical properties, such as high elasticity, tensile strength, and crack growth resistance. NR is one of the most important natural materials that is widely used in the rubber industry.⁸⁻¹⁰

NR comes from the *Hevea* trees. The production capacity of NR is restricted by the natural conditions of the geographical environment. Research has focused on the synthesis of its synthetic analog (cis-1,4-polyisoprene, IR). Although the backbone of IR is similar to that of NR, there are several differences between NR and IR. NR consists of 94% polyisoprene and 6% natural components including proteins (2.2%), phospholipids and neutral lipids (3.4%), carbohydrates (0.4%), metal salts and oxides (0.2%) and other materials (0.1%).^{11,12} Functional groups at both ends of the chains in NR interact with the natural components to create a naturally occurring network that improves the SIC of NR.¹³⁻¹⁵ The polyisoprene component in NR is composed of 100% cis-1,4 conformation, and the gel content of NR is larger than 20%. In contrast, IR is synthesized using Li-, Ti, and Nd-based catalyst systems.¹⁶⁻¹⁹ IR contains only polyisoprene molecules (100%). The polyisoprene component in IR contains only 92~98% of the cis-1,4 conformation, and the gel content of IR is less than 10%.^{3,13}

Due to the self-reinforcing characteristic of SIC for crystallizable rubber during stretching, the SIC characteristics of NR and IR have been extensively studied with the development of in situ synchrotron wide-angle X-ray diffraction (WAXD),^{1,20-24} in which the high intensity of WAXD enables the structural development and stress-strain relationship of rubbers to be measured without holding.^{25,26} Amnuaypornsi et al.^{14,15} and Toki et al.^{11,13} concluded that the naturally occurring network and entanglements in unvulcanized NR improved the SIC, modulus and tensile strength of NR during stretching. Tosaka et al.^{9,21} revealed that NR exhibited lower α_c and faster crystallinity than IR because the stereoregularity of IR was lower than that of NR.²⁷ Toki et al.¹³ reported that the α_c of NR and IR decreased with an increase in the temperature when the temperature was above -25 °C. Chenal et al.^{2,28} explored the effect of crosslink density (γ) on the crystallization rate of NR during stretching. They found that with increasing γ of NR, the crystallization rate of NR increased when γ was lower than 1.2×10^{-4} mol/cm³, which was governed by the nucleation of crystallites, and the crystallization rate of NR decreased when γ was higher than 1.2×10^{-4} mol/cm³, which was governed by the growth of the crystallites uniaxial deformation. It was concluded that the maximum crystallization rate was obtained when γ was approximately 1.2×10^{-4} mol/cm³. Weng et al.²⁹ studied the effect of filler on the SIC of NR. The results showed that NR filled with a small amount of multiwalled carbon nanotubes exhibited a higher crystallinity and lower α_c than NR in the absence of fillers. Ozbas et al.⁷ determined that the α_c of a NR/functionalized graphene sheet composite was lower than that of a NR/carbon black composite because the specific surface area of functionalized graphene sheets was approximately 8 times higher than that of carbon black.

In the rubber industry, plasticizers are widely used to improve the processing characteristics and reduce the cost of rubber materials.³⁰ Plasticizers have a great influence on the movement of rubber chains. Therefore, the orientation and crystallization of the rubber chains are affected by the addition of plasticizers. Mark and co-workers^{31,32} studied the effect of plasticizers on the stress-strain

isotherms of cis-1,4-polybutadiene. These studies concluded that the addition of a plasticizer suppressed the SIC of cis-1,4-polybutadiene. However, the investigation of SIC through stress-strain isotherms obtained via elongation of crystallizable networks is an indirect approach. Therefore, the onset formation of crystals cannot be accurately observed, and the crystallinity cannot be quantitatively determined. In recent years, the effects of plasticizers on the SIC of rubber vulcanizates have been rarely studied by WAXD technology, which is used to directly investigate the SIC of crystallizable rubber during uniaxial stretching.

The main topic of the present work is to analyze the SIC characteristics of NR and IR, and the effect of plasticizers—naphthenic oil (NPO) and liquid isoprene (LIR-50) on the SIC characteristics of NR and IR respectively by WAXD. The mechanical properties of NR, IR and their respective composites filled with NPO and LIR-50 have been measured. This article allows us to gain further insight into the change of α_c , the relationship between the upturn in stress and crystallinity, and the relationship of SIC and the mechanical properties. It is expected that these experimental results will provide a theoretical basis for the application of reactive plasticizers in NR and IR.

2. Experimental Section

2.1. Materials

NR (type SCR WF) was manufactured by Yunnan Natural Rubber Industrial Co., Ltd, China. IR (type IR70) was produced by Qingdao Yikesi New Material Co., Ltd, China. LIR-50 was synthesized in our lab by anionic polymerization.³³ NPO was produced by Nanjing Yangtze Petrochemical Co., Ltd, China. The other rubber additives, such as zinc oxide, stearic acid, and sulfur, were of commercial grade. The structural parameters of NR, IR and LIR are listed in Table 1.

Insert Table 1

2.2 Formulation for rubber compounds

Insert Table 2

Other ingredients of the formulations are as follows: zinc oxide 4.0, stearic acid 2.0, N-cyclohexyl-2-benzothiazylsulfenamide 1.2, poly(1,2-dihydro-2,2,4-trimethylquinoline) 1.0, N-isopropyl-N'-phenyl-p-phenylenediamine 1.0, sulfur 2.25 (phr)^e. ^e Parts-per-hundred rubber.

2.3 Specimen preparation

2.3.1 Preparation of rubber compounds

NR was first masticated by a $\Phi 360 \times 900$ mm two-roll mill (Shanghai Rubber Machinery Works No) for 3 min. Then, zinc oxide and other ingredients were added to these samples and mixed for 3 min to form NR compounds. IR was first masticated for 0.5 min. Other ingredients were added to these samples and mixed for 3 min to form IR compounds.

2.3.2 Preparation of vulcanizates

The vulcanizing properties of the compounds were determined by a P3555B₂ Disc Vulkameter (Beijing Huanfeng Chemical Machinery Trial Plant, Beijing, China). The vulcanizates were prepared in an XLB-D350 \times 350 plate vulcanization machine (Huzhou Dongfang Machinery Co., Ltd., Zhejiang, China) at 145 °C for the optimum cure time t_{90} . The hydraulic pressure was 15 MPa, the thickness of the vulcanizate samples for the WAXD test and simultaneous tensile measurements was approximately 0.4 mm, and the thickness of the vulcanizate samples for the mechanical test was 2.0 mm.

2.4 Characterization

The number-average molecular weight (M_n) and polydispersity index (M_w/M_n) of the raw materials were measured by gel permeation chromatography (Waters 150-C, Waters Co., Ltd. USA). LIR-50 was dissolved in tetrahydrofuran (THF) at a concentration of about 1 mg/mL for 1 day. IR was cut into small pieces and dissolved in THF at a concentration of about 1 mg/mL for 1 day. Because of high molecular weight, and high content of branching and microgels in raw NR, NR was

cut into pieces and dissolved in THF at a concentration of about 1 mg/mL for 7 days. Furthermore, all rubber solutions were filtrated in PTFE membranes with a membrane pores size of 0.45 μm , and then injected into the GPC system using a 1.0 mL/min flow rate at 30 $^{\circ}\text{C}$.

The mechanical properties were measured according to ASTM D412-06 by CMT4104 Electrical Tensile Tester (Shenzhen SANS Test Machine Co., Ltd. China) at a tensile rate of 500 mm/min. Shore A hardness was determined according to ASTM D2240-05 on a Shore A durometer (Heinrich BAREISS GmbH, Oberdischingen, Germany). The resilience test was performed on a MZ-4065 Resilience Elasticity Tester (Mingzhu Testing Machinery Co., Ltd, China) according to ASTM D2632-01.

The stress relaxation test was carried out according to ASTM D 674 standard. A relaxation test apparatus was designed and assembled for the purpose of testing the relaxation behavior of rubber materials. Relaxation curves for all samples were recorded at a strain= 350% at 20 $^{\circ}\text{C}$ for 2000 s.

The crosslink density (γ) of the vulcanized rubber was carried out with a swelling method. The vulcanized rubber samples were immersed in n-hexane at 30 $^{\circ}\text{C}$ for 7 days. Then the excess liquid on the surface of the specimens was removed quickly by blotting them with filter paper. The specimens were weighted in a weighting bottle and then dried in a vacuum oven at 50 $^{\circ}\text{C}$ for 2 days. The weight of the dried samples was then measured. The γ of the vulcanizates was calculated from the swelling ratio by the Flory-Rehner equation (1):

$$-\left[\ln(1 - v_2) + v_2 + x_1 v_2^2\right] = V_1 \gamma \left[v_2^{1/3} - \frac{v_2}{2} \right], \quad (1)$$

where v_2 is the volume fraction of polymer in the swollen mass, V_1 (130.7 cm^3/mol) is the molar volume of the solvent (n-hexane), and x_1 is the Flory-Huggins polymer-solvent dimensionless interaction term (x_1 is equal to 0.5 for the system NR-n-hexane).

The solvent extraction rate of the vulcanizates was determined by a Soxhlet apparatus at 80 $^{\circ}\text{C}$.

N-hexane was used as the solvent, and the extraction time was 120 h. The extracted samples were dried in a vacuum to a constant weight (m_1) at 50 °C. The n-hexane extraction rate was calculated using equation (2):

$$\text{Extraction rate (\%)} = (m_2 - m_1)/m_2 \times 100, \quad (2)$$

where m_2 is the weight of the sample before the extraction test.

In situ synchrotron WAXD measurements were carried out at the 1W2A beamline in the Beijing Synchrotron Radiation Facility (BSRF) at the Institute of High Energy Physics Chinese Academy of Sciences. The wavelength of the X-ray used was 1.54 Å. Two-dimensional WAXD patterns were recorded by a MAR 165 CCD detector for quantitative image analysis. The typical image exposure time was 20 s, and the sample-to-detector distance was 182 mm. The experiments were carried out at room temperature (approximately 22 °C). The specimen was a rectangular sheet with 25×6×0.4 mm. A Linkam tensile tester, which allowed for symmetric deformation of the sample, was used for the in situ WAXD study. The original distance between the clamps was 15 mm, and the deformation rate was 10 mm/min. The stress (σ) was measured as $\sigma = F/d_0\omega_0$, where F is the force measured by a load cell, d_0 is the initial thickness, and ω_0 is the initial width of the sample. In terms of the deformation ratio, the strain (α) was given by $\alpha = (l - l_0)/l_0$, where l_0 is the original clamp-clamp distance and l is the extended clamp-clamp distance during deformation. Due to the limitation of the Linkam tensile tester, the maximum distance of between the clamps was 95 mm. Therefore, for the WAXD test, the maximum strain was about 530% where all samples were not broken up. The time-resolved WAXD patterns and simultaneous stress–strain relationship were continuously recorded without holding the sample in still conditions during stretching.

2.5 Processing of the WAXD data

In this research, air scattering was subtracted from all the WAXD patterns for further analysis using the Fit2D software package. The diffraction intensity near the meridian was normalized and

azimuthally integrated in a cake from 75° to 105°, as shown in Figure 1. For example, Figure 1 represented the cake-integrated intensity as a function of the 2θ for NR at 483% strain. The resulting profiles were deconvoluted considering the diffraction peaks of the 200 and 120 planes and the amorphous halo using the Peak Analyzer software.⁸ The mass fraction crystallinity index (X_c) at room temperature was estimated from diffraction intensity data ($2\theta=5\sim 25^\circ$) using equation (3):

$$X_c(\%) = A_c / (A_c + A_a) \times 100, \quad (3)$$

where A_c is the area below the 200 and 120 crystalline peaks and A_a is the area below the amorphous halo. The crystallinity of WAXD pattern was not calculated when X_c was less than 0.5%.

Insert Figure 1

3. Results and Discussion

3.1 SIC behaviors of NR and IR

The stress-strain curves and crystallinity of NR and IR during stretching are shown in Figures 2 and 3.

Insert Figure 2

As shown in Figure 2, the WAXD patterns of NR and IR at $\alpha = 0$ exhibit an isotropic amorphous halo with no preferred orientation. As the strain increased, the stress of NR and IR increases, and the stress of NR is higher than that of IR. The α_c of NR and IR is 250% and 350% respectively. NR has a smaller α_c than IR. NR and IR exhibit a stress upturn at approximately 383% and 450%, respectively, and their corresponding WAXD patterns exhibit an oriented crystal pattern.

Insert Figure 3

The results in Figure 3 shows that with increasing strain the crystallinity of NR and IR increases rapidly when $\alpha > \alpha_c$, and the crystallinity of NR is higher than that of IR. At the point of the

upturn in stress, the crystallinity of NR and IR is about approximately 7.6% and 8.6%, respectively. Therefore, when the crystallinity of NR or IR is approximately 8%, the contribution of crystals to reinforcement of NR or IR vulcanizates increases, and so the stress upturns indicating a “self-reinforcement” feature. NR has a naturally occurring network and the stereoregularity of NR is higher than that of IR. During stretching the naturally occurring network acts as constraints in order to align molecules to induce crystals during deformation.¹³ Compared with IR, the higher stereoregularity of NR is also benefit to the SIC of NR. Therefore, NR has a higher SIC characteristic leading to higher crystallinity and stress than IR.

3.2 Effect of plasticizers on the curing characteristic and extraction rate of NR and IR

Table 3 shows the effect of plasticizers on the curing characteristic and extraction rate of NR and IR.

Insert Table 3

It can be seen from Table 3 that the scorch time (t_{10}) and optimum cure time (t_{90}) for NR and IR increase slightly, and the crosslink density (γ) decreases after the addition of NPO and LIR-50. NR (NR-0~NR-2) exhibits shorter t_{10} and t_{90} , and higher γ than IR (IR-0~IR-2) because the proteins and stearic acid, which are inherently contained in NR, can accelerate the vulcanization of NR.^{34, 35}

The extraction rate of NR composites is higher than that of IR composites, indicating that NR composites contain a certain amount of inherent removable stearic acid and proteins. After the addition of NPO, the extraction rate of NR composites and IR composites increases significantly respectively, and approximately 97% of NPO molecules are extracted from the rubber networks, indicating that NPO exists as free small molecules in the rubber networks. There are repeating double bonds in the main chains of LIR-50, NR and IR. After the addition of LIR-50, the extraction rate of NR and IR barely changes, indicating that the molecules of LIR-50 and rubber are linked through the sulfur crosslinks during vulcanization. LIR-50 becomes part of the rubber networks.³⁶

3.3 Effect of plasticizers on the SIC characteristics and stress relaxation of NR and IR

The effect of NPO and LIR-50 on the stress-strain curves of NR and IR respectively is shown in Figure 4.

Insert Figure 4

The first WAXD pattern of each sample is the first pattern with oriented crystal reflection during the WAXD test. The second WAXD pattern of each sample (except sample IR-1) is near the upturn in the stress. As shown in Figure 4(a), after the addition of NPO to NR, the stress decreases, and the α_c barely changes (i.e., approximately 250%). The strain of stress upturn increases to 410%, and the WAXD pattern near the strain of stress upturn exhibits an apparent oriented crystal pattern. However, after the addition of NPO to IR, the stress decreases significantly, the α_c shifts from 350% (IR-0) to 417% (IR-1) and there is no apparent upturn in the stress. The results in Figure 4(b) indicate that after the addition of LIR-50 to NR, the stress also decreases, and the α_c is 250%. The strain of stress upturn is approximately 405%, and the corresponding WAXD pattern also exhibits an apparent oriented crystal pattern. The effect of LIR-50 on the stress-strain curve of NR is similar to that of NPO. After the addition of LIR-50 to IR, the stress also decreases, and the α_c shifts from 350% to 383%. In addition, IR/LIR-50 composite exhibits an upturn in stress, and the strain of stress upturn increases to 470%.

Insert Figure 5

Figure 5 shows the effect of NPO and LIR-50 on the crystallinity of NR and IR. As shown in Figure 5(a), the crystallinity of NR decreases after the addition of NPO or LIR-50, and the reduction of crystallinity of NR plasticized by NPO is more obvious. At the strain of stress upturn, the crystallinity of NR, NR/NPO and NR/LIR-50 is approximately 7.6%, 8.1% and 8.4%, respectively.

The results in Figure 5(b) indicate that after the addition of NPO or LIR-50, the crystallinity of IR significantly decreases, and the reduction of crystallinity of IR/NPO is higher than that of IR/LIR-50. The crystallinity of IR/NPO is only approximately 3.8% at 517% strain. Therefore, the stress does not upturn in Figure 4(a).

Insert Figure 6

Figure 6 shows the effect of NPO and LIR-50 on the stress relaxation of NR and IR. Figure 6 shows that the normalized relaxation stresses, $\sigma(t)/\sigma(0)$, of NR and IR decrease after the addition of NPO or LIR-50. Moreover, $\sigma(t)/\sigma(0)$ of NR or IR plasticized by NPO is lower than that plasticized by LIR-50, i.e., the stress relaxation of NR or IR plasticized by NPO is faster than that plasticized by LIR-50, illustrating that LIR-50 links to the molecular chains of rubber networks and NPO exists as small molecules.

The stress relaxation of NR and IR composites is an important factor affecting the formation and growth of crystals during stretching. As shown in Figure 7, after vulcanization, LIR-50 links to the molecular chains of NR and IR, and the stress relaxation of these vulcanizates increases slightly. However, NPO exists as free small molecules in rubber networks and increases the stress relaxation speed of these vulcanizates apparently. The stress-relaxation time of rubber chains plasticized by NPO becomes shorter and the force subjected to these chains reduces rapidly, which hinders the orientation of these rubber chains under stress and the formation of crystals. Therefore, as the stretching samples in Figure 6, the suppressing effect of NPO on the SIC of NR and IR is higher than that of LIR-50.

Insert Figure 7

Based on a comparison of the results in Figures 5(a) and 5(b), the suppressing effect of these plasticizers on the SIC of NR is lower than that of IR. After incorporation of NPO or LIR-50, the reduction of crystallinity of NR is much lower than that of IR. In addition, the α_c of NR barely

changes, while the α_c of IR increases. The different behavior of NR and IR may be caused by the higher stereoregularity and naturally occurring network of NR. The entanglements of the naturally occurring network become pivots for aligning the amorphous chains into crystalline order and reducing the effect of plasticizers on the stress relaxation of the molecular chains.^{11,13}

3.4 Effect of plasticizers on the mechanical properties of NR and IR

The mechanical properties of NR and IR filled with NPO and LIR-50 respectively are shown in Table 4.

Insert Table 4

After the incorporation of NPO and LIR-50, the Shore A hardness and modulus at 300% of NR and IR decreases, and the elongation at break (EB) increases, which are both due to the decrease in the crosslink density. The reduction of hardness of NR and IR plasticized by LIR-50 is lower than that plasticized by NPO. The rebound resilience of NR and IR barely changes. The tensile strength (TS) of NR and IR decreases. The TS and the EB of NR and IR plasticized by NPO are lower than those plasticized by LIR-50. In particular, compared with the TS of IR vulcanizate, the TS of IR plasticized by LIR-50 reduced by 11%, while the TS of IR plasticized by NPO reduced by 37%.

In comparison with the data in Table 4 and Figure 5, we can conclude that the addition of NPO and LIR-50 suppresses the SIC of NR and IR. Therefore, the TS of these vulcanizates decreases. The reduction in the crystallinity of NR and IR plasticized by NPO is higher than that plasticized by LIR-50. Therefore, NR and IR plasticized by NPO have a lower TS and EB. The SIC characteristics of NR and IR have a substantial influence on their final properties.

4. Conclusions

In situ synchrotron WAXD during stress-strain measurements have been performed on NR, IR and their plasticized samples. First, it was observed that NR had lower α_c and higher crystallinity

than IR during stretching. Secondly, after the addition of plasticizers, the SIC of NR and IR was suppressed, and the suppressing effect of plasticizers on the SIC of NR was lower than that of IR. The existence of a naturally occurring network could play a very important role in the SIC of NR compared with IR before or after the addition of plasticizers. In addition, the suppressing effect of NPO on the SIC of NR and IR was higher than that of LIR-50 due to the different existing states and structures of these plasticizers. During stretching, the stress upturned when the crystallinity was about 8% for NR and IR, even for the plasticized samples, because the contribution of self-reinforcement of the strain-induced crystals was more apparent when the crystallinity attained a critical value.

Through mechanical tests, we found that the tensile strength of NR and IR decreased after incorporation of the NPO and LIR-50. The tensile strength and the elongation at break of NR and IR plasticized by LIR-50 were higher than those plasticized by NPO. LIR-50 is more suitable for use as a reactive plasticizer in NR and IR. The SIC characteristic is an important factor affecting the final properties of NR and IR.

Nomenclature

WAXD	In synchrotron wide-angle X-ray diffraction
LIR-50	Liquid isoprene with M_n of about 50,000
M_n	Number-average molecular weight
M_w	Weight-average molecular weight
SIC	Strain-induced crystallization
α_c	Onset strain of crystallization
IR	Synthetic polyisoprene
M_w/M_n	Polydispersity index
EB	Elongation at break
t_{90}	Optimum cure time
γ	Crosslink density
TS	Tensile strength

m:s	Minute:second
NR	Natural rubber
NPO	Naphthenic oil
t ₁₀	Scorch time
α	Strain

Acknowledgments

The authors acknowledge financial support from the Beijing Synchrotron Radiation Facility (BSRF), Institute of High Energy Physics Chinese Academy of Sciences. Prof. Guang Mo and Prof. Zhihong Li of BSRF are warmly thanked for their help with the synchrotron WAXD experiments.

References

1. J. Che, C. Burger, S. Toki, L. Rong, B. S. Hsiao, S. Amnuaypornsrri and J. Sakdapipanich, *Macromolecules*, 2013, **46**, 4520-4528.
2. J.-M. Chenal, L. Chazeau, L. Guy, Y. Bomal and C. Gauthier, *Polymer*, 2007, **48**, 1042-1046.
3. S. Toki, I. Sics, S. Ran, L. Liu and B. S. Hsiao, *Polymer*, 2003, **44**, 6003-6011.
4. M. Tosaka, S. Murakami, S. Poompradub, S. Kohjiya, Y. Ikeda, S. Toki, I. Sics and B. S. Hsiao, *Macromolecules*, 2004, **37**, 3299-3309.
5. Y. Fukahori, *Polymer*, 2010, **51**, 1621-1631.
6. B. J. Zhao, N. Tian, Y. P. Liu, T. Z. Yan, W. Q. Zhou, L. B. Li, Y. G. Zhou, G. S. Weng and G. S. Huang, *J. Polym. Sci. Part B: Polym. Phys.*, 2012, **50**, 1630-1637.
7. B. Ozbas, S. Toki, B. S. Hsiao, B. Chu, R. A. Register, I. A. Aksay, R. K. Prud'homme and D. H. Adamson, *J. Polym. Sci. Part B: Polym. Phys.*, 2012, **50**, 718-723.
8. M. Hernández, M. A. López-Manchado, A. Sanz, A. Nogales and T. A. Ezquerro, *Macromolecules*, 2011, **44**, 6574-6580.

9. M. Tosaka, D. Kawakami, K. Senoo, S. Kohjiya, Y. Ikeda, S. Toki and B. S. Hsiao, *Macromolecules*, 2006, **39**, 5100-5105.
10. T. Kawazura, S. Kawahara and Y. Isono, *J. Appl. Polym. Sci.*, 2005, **98**, 613-619.
11. S. Toki, B. S. Hsiao, S. Amnuaypornsi and J. Sakdapipanich, *Polymer*, 2009, **50**, 2142-2148.
12. S. Toki, C. Burger, B. S. Hsiao, S. Amnuaypornsi, J. Sakdapipanich and Y. Tanaka, *J. Polym. Sci. Part B: Polym. Phys.*, 2008, **46**, 2456-2464.
13. S. Toki, J. Che, L. Rong, B. S. Hsiao, S. Amnuaypornsi, A. Nimpai boon and J. Sakdapipanich, *Macromolecules*, 2013, **46**, 5238-5248.
14. S. Amnuaypornsi, *Rubber Chem. Technol.*, 2008, **81**, 753-766.
15. S. Amnuaypornsi, S. Toki, B. S. Hsiao and J. Sakdapipanich, *Polymer*, 2012, **53**, 3325-3330.
16. S. Kaita, Y. Doi, K. Kaneko, A. C. Horiuchi and Y. Wakatsuki, *Macromolecules*, 2004, **37**, 5860-5862.
17. W. M. Dong and T. Masuda, *J. Polym. Sci., Polym. Chem.*, 2002, **40**, 1838.
18. Z. Q. Shen, J. Ouyang, F. S. Wang, Z. Y. Hu, F. S. Yu and B. G. Qian, *J Polym Sci Part A: Polym Chem.*, 1980, **18**, 3345.
19. H. L. Hsieh and H. C. Yeh, *Rubber Chem. Technol.*, 1984, **58**, 117.
20. S. Toki, I. Sics, B. S. Hsiao, S. Murakami, M. Tosaka, S. Poompradub, S. Kohjiya and Y. Ikeda, *J. Polym. Sci. Part B: Polym. Phys.*, 2004, **42**, 956-964.
21. M. Tosaka, S. Kohjiya, S. Murakami, S. Poompradub, Y. Ikeda, S. Toki, I. Sics and B. S. Hsiao, *Rubber Chem. Technol.*, 2004, **77**, 711-723.
22. S. Poompradub, M. Tosaka, S. Kohjiya, Y. Ikeda, S. Toki, I. Sics and B. S. Hsiao, *J. Appl. Phys.*, 2005, **97**, 103529/1-103529/9.
23. S. Kohjiya, M. Tosaka, M. Furutani, Y. Ikeda, S. Toki and B. S. Hsiao, *Polymer*, 2007, **48**, 3801-3808.

24. S. Toki, R. Takagi, M. Ito and B. S. Hsiao, *Polymer*, 2011, **52**, 2453-2459.
25. Z. H. Li, Z. H. Wu, G. Mo, X. Q. Xing and P. Liu, *Instrum. Sci. Technol.*, 2014, **42**, 128-141.
26. Z. H. Li, *Chinese Phys. C*, 2013, **37**, 108002/1-108002/6.
27. A. N. Gent, S. Kawahara and J. Zhao, *Rubber Chem. Technol.*, 1998, **71**, 668-678.
28. J.-M. Chenal, C. Gauthier, L. Chazeau, L. Guy and Y. Bomal, *Polymer*, 2007, **48**, 6893-6901.
29. G. S. Weng, G. S. Huang, L. L. Qu, Y. J. Nie and J. R. Wu, *J. Phys. Chem. B*, 2010, **114**, 7179-7188.
30. A. Ciesielski, *An Introduction to Rubber Technology*, Rapra Technology Ltd., Shawbury, Shrewsbury, Shropshire, UK, 1999.
31. J. E. Mark, *Polym. Eng. Sci.*, 1979, **19**, 409-413.
32. D. S. Chiu, T. K. Su and J. E. Mark, *Macromolecules*, 1977, **10**, 1110-1116.
33. Q. Q. Li, M.S. Thesis, Beijing University of Chemical Technology, Beijing, China, 2013.
34. S. Amnuaypornsrri, J. Sakdapipanich and Y. Tanaka, *J. Appl. Polym. Sci.*, 2010, **118**, 3524-3531.
35. K. Siti Maznah, A. Baharin, I. Hanafi, M. E. Azhar and M. H. Mas Rosemal Hakim, *Polym. Test.*, 2008, **27**, 1013-1016.
36. Y. Q. Ren, S. H. Zhao, Q. Q. Li, X. Y. Zhang, L. Q. Zhang, *J. Appl. Polym. Sci.*, 2014, DOI: 10.1002/app.41485.

Tables

Table 1. Structural parameters of NR, IR and LIR

	NR	IR	LIR-50
M_n (g/mol)	390,000	333,000	48,000
M_w/M_n	2.47	3.07	1.23
cis-1,4 ^a (%)	99.90	92.81	71.29
trans-1,4 ^a (%)	0.10	3.39	21.73

3,4- ^a (%)	-	3.79	6.98
-----------------------	---	------	------

^a Percentage of cis-1,4, trans-1,4 and 3,4- units in raw materials.

Table 2. Formulations of the NR and IR compounds

Sample no.	NR-0	NR-1	NR-2	IR-0	IR-1	IR-2
NR (phr)	100	100	100			
IR (phr)				100	100	100
NPO (phr)		10			10	
LIR-50 (phr)			10			10

Table 3. Curing characteristic and extraction rate of NR/plasticizer and IR/plasticizer composites

	NR-0	NR-1	NR-2	IR-0	IR-1	IR-2
t ₁₀ (m:s)	8:34	8:56	8:48	15:21	17:11	16:12
t ₉₀ (m:s)	13:43	14:15	14:07	20:06	23:22	21:06
γ (*10 ⁴ mol/cm ³)	3.17	2.68	2.55	2.32	1.94	1.97
Extraction rate (%)	5.62	13.20	5.79	3.77	11.50	3.70

Table 4. Mechanical properties of NR and IR plasticized by NPO and LIR-50, respectively

	NR-0	NR-1	NR-2	IR-0	IR-1	IR-2
Shore A hardness	44.2	40.0	43.3	39.9	36.9	38.6
Rebound resilience (%)	81.0	80.8	79.4	81.0	80.8	79.0
Modulus at 300% (MPa)	3.4	2.8	2.6	2.5	1.9	2.0
TS (MPa)	29.7	24.4	27.0	24.3	15.3	21.7
EB (%)	649	660	715	644	660	710

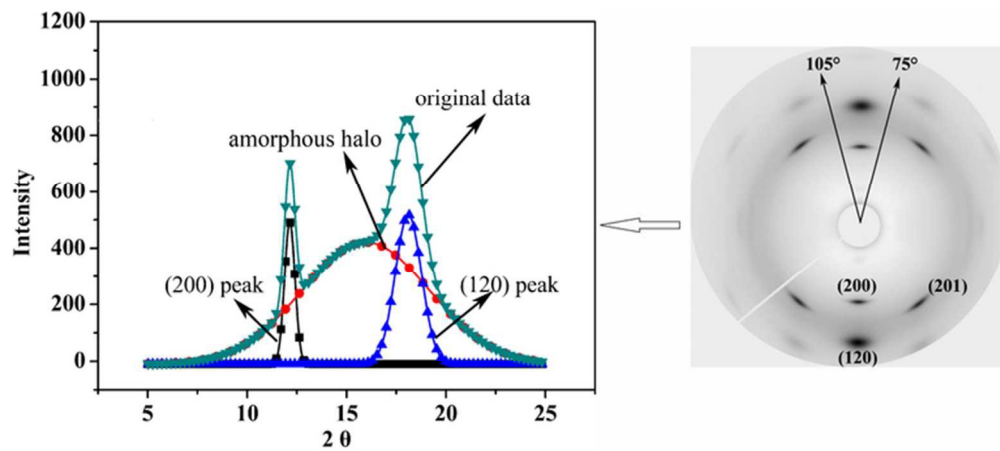


Figure 1. Meridional cake-integrated intensity as a function of the 2θ taken from the WAXD pattern of the stretched vulcanized NR (A11) at $\alpha = 483\%$. The inset shows the integration limits from 75° to 105° .
64x28mm (300 x 300 DPI)

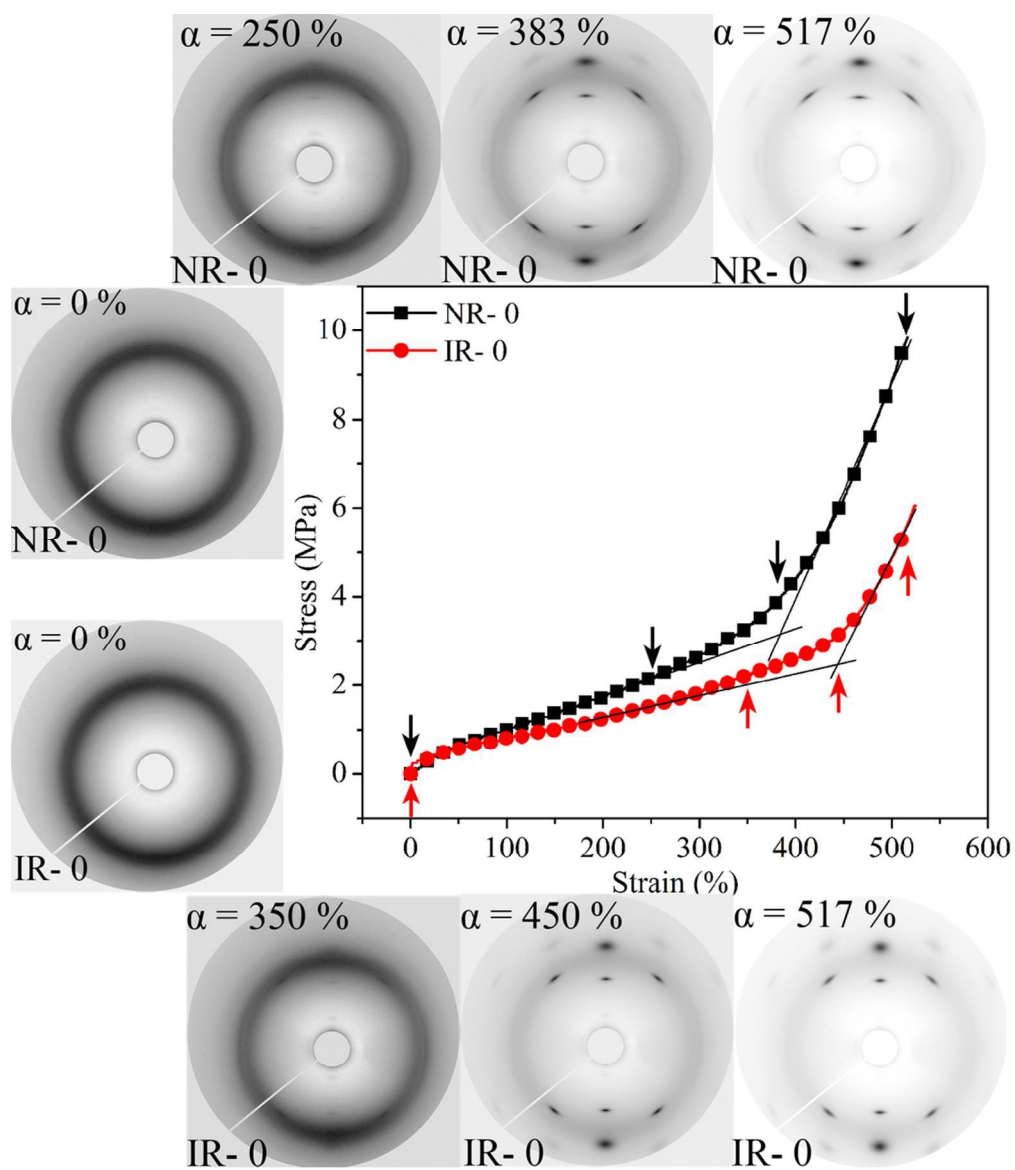


Figure 2. Stress-strain curves and selected WAXD patterns collected during stretching of NR and IR. 95x110mm (300 x 300 DPI)

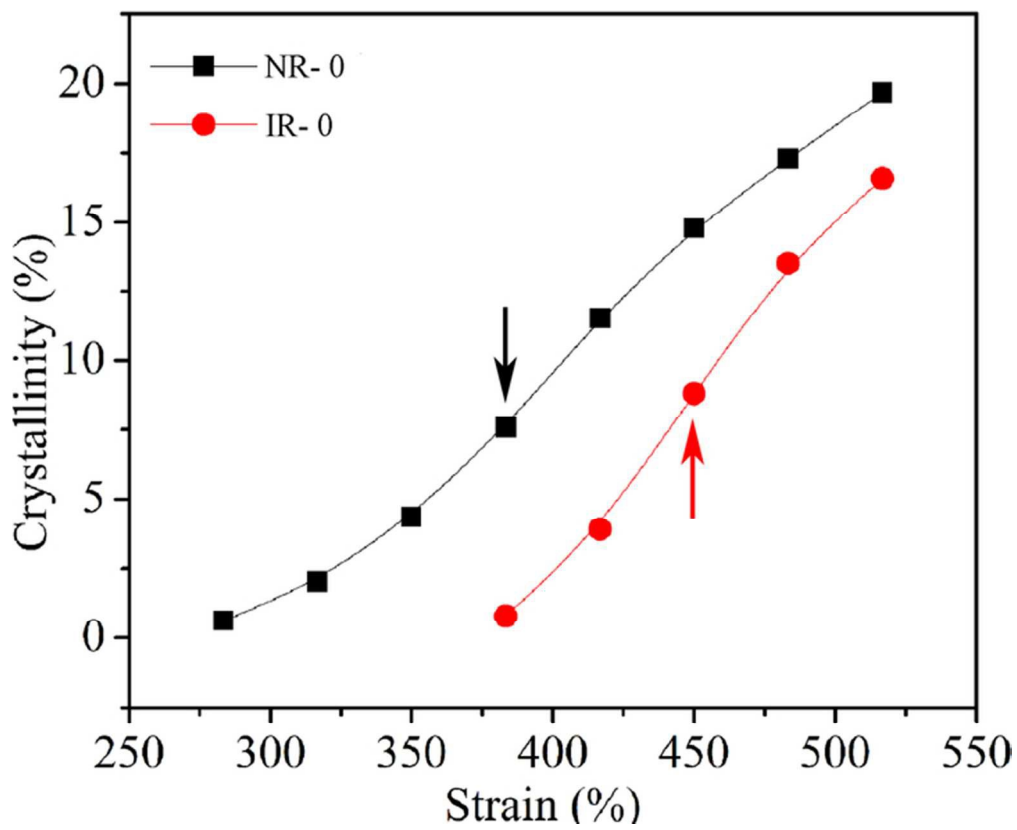


Figure 3. Variation of crystallinity of NR and IR with strain.
60x49mm (300 x 300 DPI)

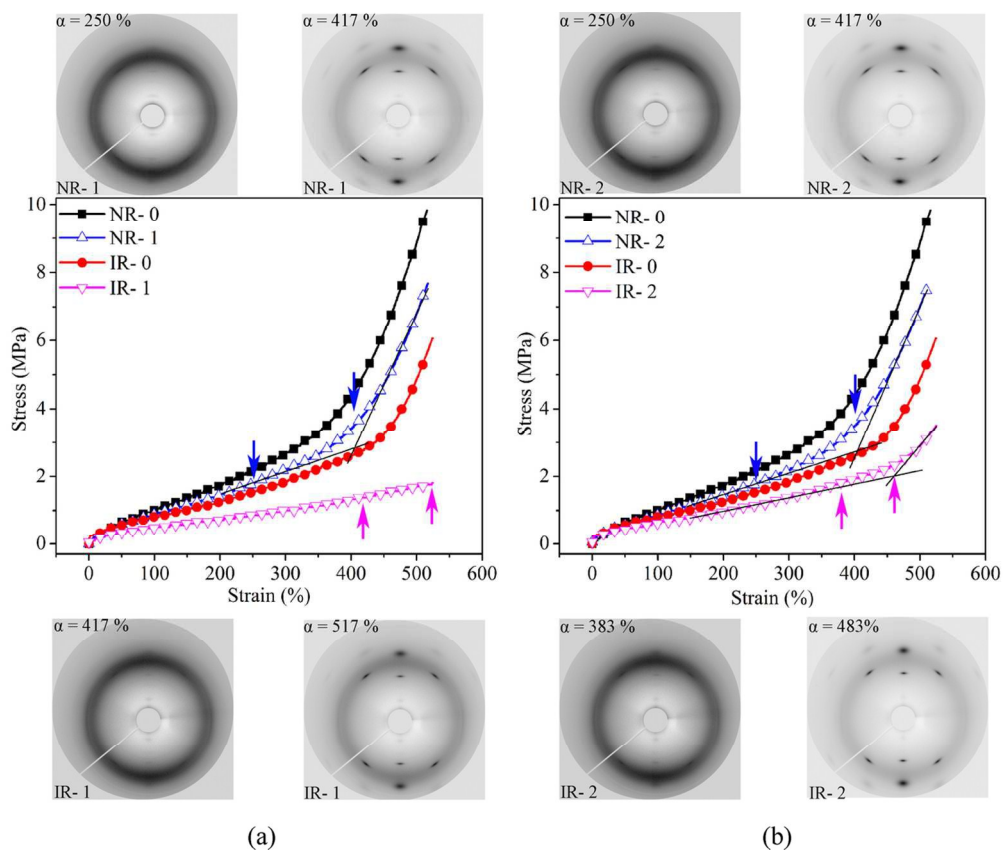


Figure 4. Stress-strain curves and selected WAXD patterns of NR and IR plasticized by (a) NPO and (b) LIR-50.
115x96mm (300 x 300 DPI)

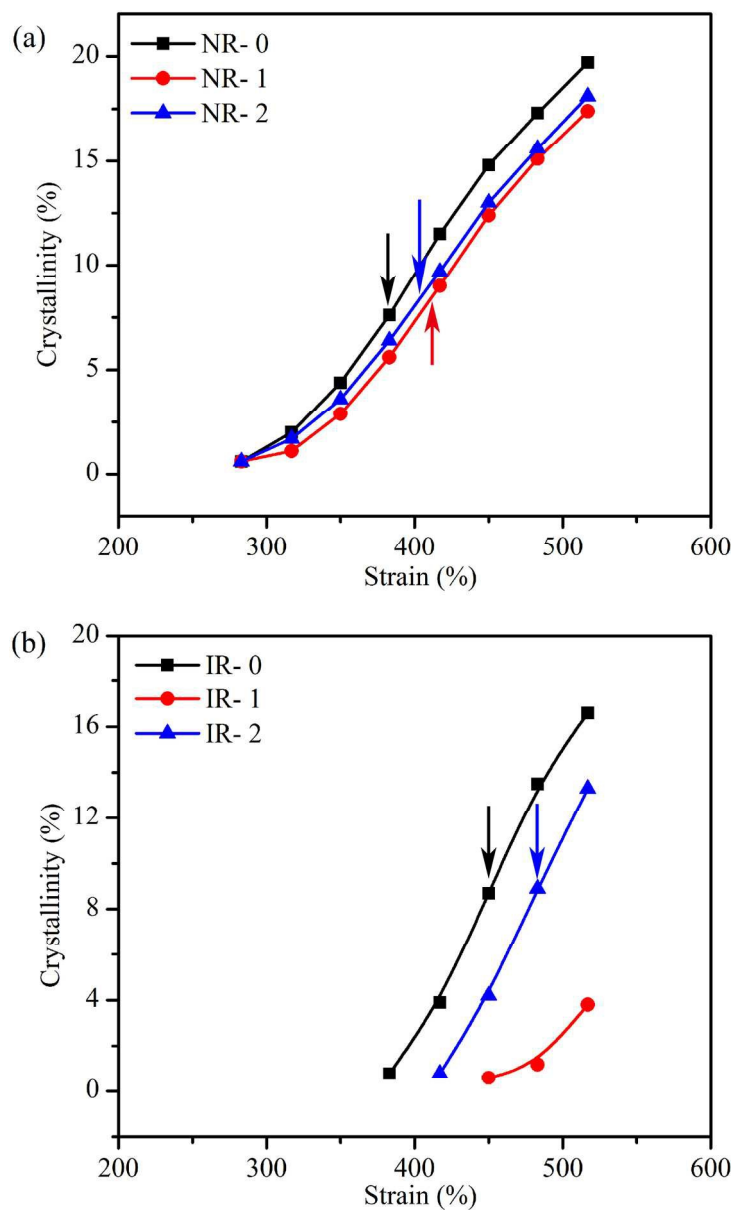


Figure 5. Effect of NPO and LIR-50 on the crystallinity of NR (a) and IR (b), respectively.
133x221mm (300 x 300 DPI)

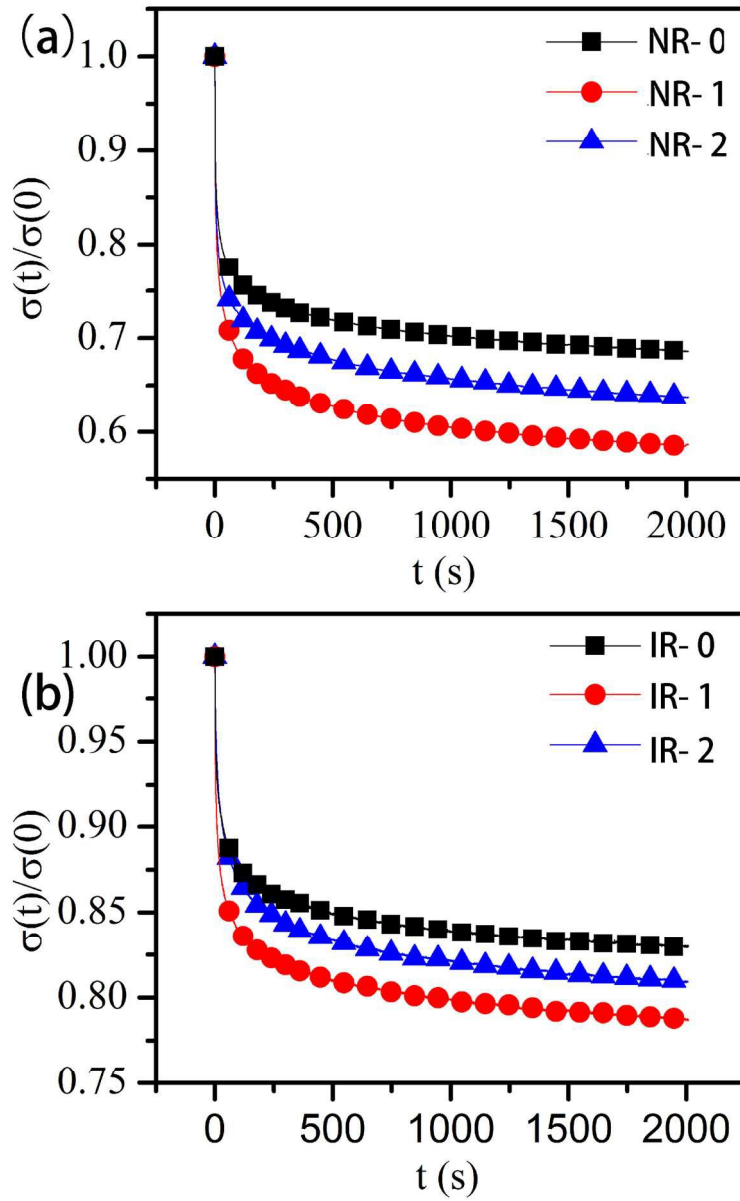


Figure 6. Normalized relaxation stresses, $\sigma(t)/\sigma(0)$, versus time for of NR and IR vulcanizates plasticized by NPO and LIR-50.
128x207mm (300 x 300 DPI)

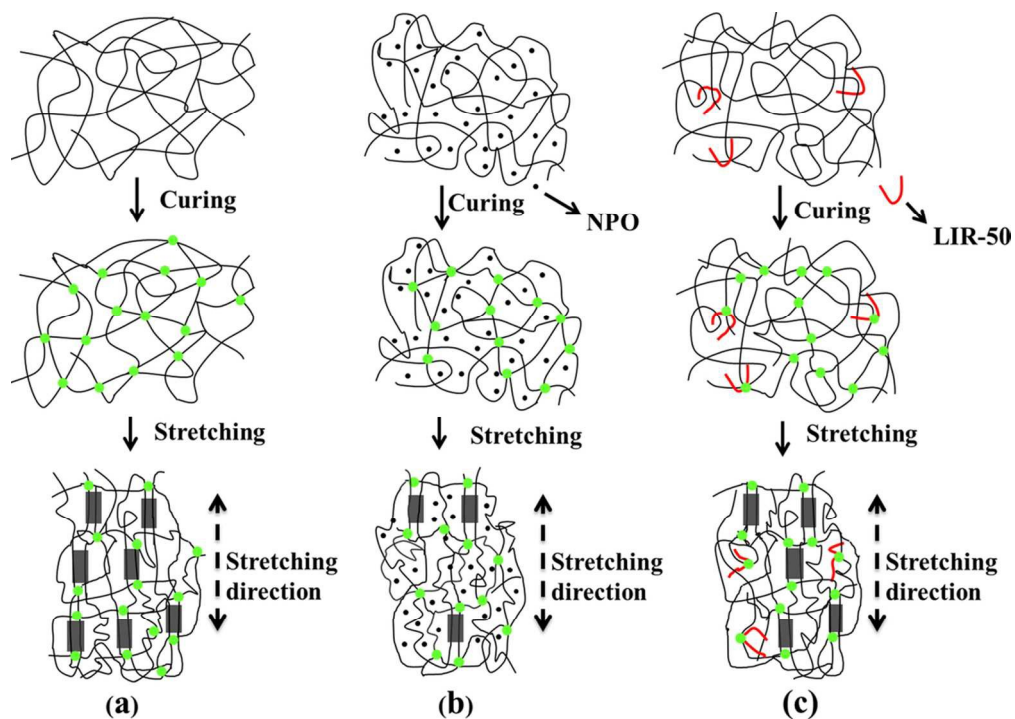
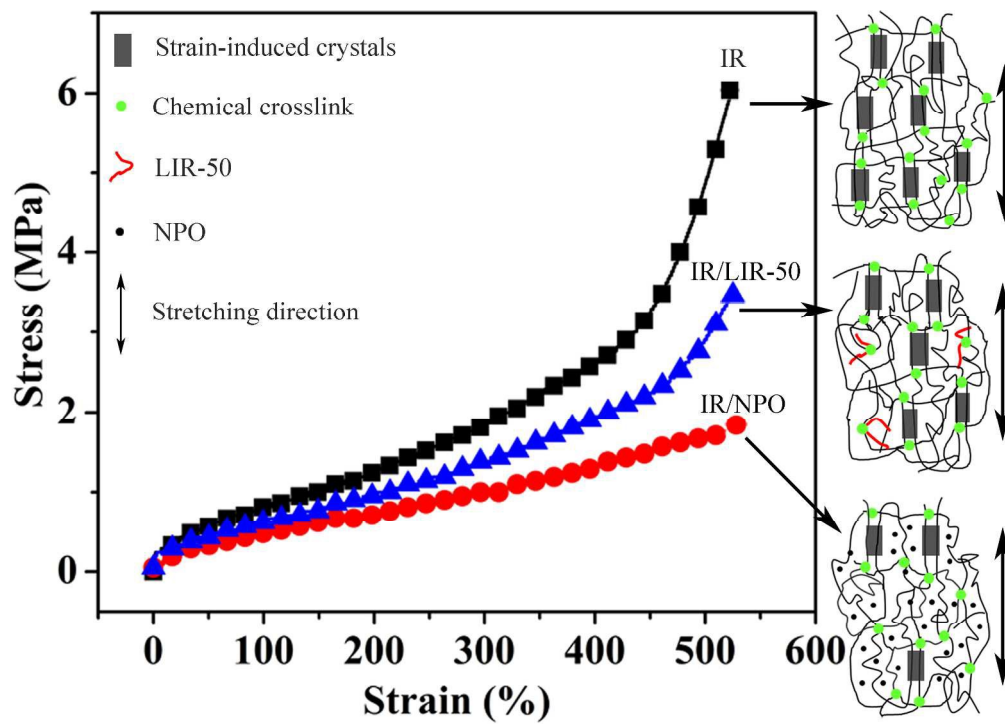


Figure 7. Schematic models of the effect of NPO (b) and LIR-50 (c) on the SIC of crystallizable rubber. Chemical crosslink (green circle), NPO (black circle), LIR-50 (red curve) and SIC (gray rectangle). 98x70mm (300 x 300 DPI)



Effects of different type of plasticizers on the strain-induced crystallization and stress-strain curves of crystallizable rubber.
242x172mm (300 x 300 DPI)